Three-dimensional colloidal crystals in liquid crystalline blue phases

Miha Ravnik[a,b], Gareth P. Alexander[b,c], Julia M. Yeomans[b], and Slobodan Žumer[a,d,1]

[a]Faculty of Mathematics and Physics, University of Ljubljana, 1000 Ljubljana, Slovenia; [b]Rudolf Peierls Centre for Theoretical Physics, University of Oxford, Oxford OX1 3NP, United Kingdom; [c]Department of Physics and Astronomy, University of Pennsylvania, Philadelphia, PA 19104; and [d]Jožef Stefan Institute, 1000 Ljubljana, Slovenia

Edited* by Noel A. Clark, University of Colorado at Boulder, Boulder, CO, and approved January 21, 2011 (received for review October 26, 2010)

Applications for photonic crystals and metamaterials put stringent requirements on the characteristics of advanced optical materials, demanding tunability, high Q factors, applicability in visible range, and large-scale self-assembly. Exploiting the interplay between structural and optical properties, colloidal lattices embedded in liquid crystals (LCs) are promising candidates for such materials. Recently, stable two-dimensional colloidal configurations were demonstrated in nematic LCs. However, the question as to whether stable 3D colloidal structures can exist in an LC had remained unanswered. We show, by means of computer modeling, that colloidal particles can self-assemble into stable, 3D, periodic structures in blue phase LCs. The assembly is based on blue phases providing a 3D template of trapping sites for colloidal particles. The particle configuration is determined by the orientational order of the LC molecules: Specifically, face-centered cubic colloidal crystals form in type-I blue phases, whereas body-centered crystals form in type-II blue phases. For typical particle diameters (approximately 100 nm) the effective binding energy can reach up to a few 100 k_BT, implying robustness against mechanical stress and temperature fluctuations. Moreover, the colloidal particles substantially increase the thermal stability range of the blue phases, for a factor of two and more. The LC-supported colloidal structure is one or two orders of magnitude stronger bound than, e.g., water-based colloidal crystals.

3D self-assembly | colloids | chirality | mesoscopic modeling

The major limitation of self-assembly approaches to building 3D photonic materials (1–6) is the difficulty of scaling the materials up from the nanoscale to the device dimensions. The approaches typically rely on the manipulation of particles by van der Waals or screened electrostatic forces (7) and the manipulation proceeds either under ultra high vacuum conditions or in water dispersions. The technological complexity lies in controlling these forces over macroscopic length scales. Technologies for 3D self-assembly are developed, based on electrically driven particle manipulation (8), sedimentation (9), growth on patterned surfaces (10), tuning of electrostatic interactions between oppositely charged particles (11, 12), and DNA-guided crystallization (13). In liquid crystal colloids, the self-assembly is demonstrated for two-dimensional structures of clusters, chains, and two-dimensional crystals (14–17). There have been recent advances in the synthesis and characterization of building blocks, but these have not been matched by similar progress in organizing the building blocks into assemblies and materials (18). Therefore, using cholesteric blue phases represents a unique and clear route to the 3D self-assembly of colloids. Recently, blue phases are receiving greater attention because materials with a broad stability range have been discovered (19, 20). In addition application of a polymer-stabilized blue phase enabled development of a display with a very fast response (21). Also, blue phases are attracting broader attention because of growing interest in condensed matter systems with analogous topological structures. One of the more interesting topological structures are chiral ferromagnets such as recently discussed MnSi (22). The main advantages of using blue phases for colloidal assembly are (*SI Text*) (*i*) highly regular large-scale trapping potentials, (*ii*) strong potentials that hold particles in trapping sites, (*iii*) simple control of the colloidal crystal via restructuring of the liquid crystal under external fields, and (*iv*) possible use of already developed assembly techniques from nonliquid crystal-based colloidal materials.

Cubic blue phases (BPs) form in highly chiral liquid crystals where rod-like molecules align in a periodic 3D orientational texture with cubic symmetry (*SI Text*). Depending on temperature, two distinct textures form, known as BP I and BP II. The texture of blue phases can be thought of as being made of stacked cylindrical tubes—double-twist cylinders—where inside molecules rotate to form helical vortices (Fig. S1) (23). In the space between cylinders molecular orientations cannot extend smoothly, forming a cubic lattice of defect lines, known as disclinations. These places of molecular misalignment are the energetically most disfavored regions in blue phases. Placing particles within the disclinations replaces part of this energetically costly region with the particles' own volume, lowering the overall energy of the LC texture. The reduction in energy is of order approximately Kr, where K is an elastic constant and r is the particle radius, leading to a binding energy of several hundred k_BT for approximately 100 nm size colloids (24). Indeed, analogously, micron-sized particles were trapped in two spatial dimensions by a single disclination in nematic (25, 26), polymer particles were trapped at the defect boundaries of opposite twist domains (27), and recently stabilization of blue phases by nanoparticles (28, 29) and guest components were demonstrated (30).

The aim of this article is to show by phenomenological modeling that colloidal particles can self-assemble into stable, 3D colloidal crystals in blue phase LCs. Three-dimensional colloidal lattices are initialized according to the symmetry of intrinsic trapping sites in blue phases and then let to relax to equilibrium. Several stable lattices with different total free energies per unit cell are found in both BP I and II. The lattice with lowest free energy is face-centered cubic (FCC) in BP I and body-centered cubic (BCC) in BP II. Interestingly, when doping blue phases with colloidal particles with weak surface of particle–liquid crystal interactions (i.e., weak surface anchoring), we find that the thermal stability range of blue phases increases substantially by a factor of two or more. This increased thermal stability is explained by scaling analysis of the relevant contributions to the total free energy of blue phase colloids.

Author contributions: M.R., G.P.A., J.M.Y., and S.Z. designed research; M.R. and G.P.A. performed research; M.R., G.P.A., J.M.Y., and S.Z. analyzed data; and M.R., G.P.A., J.M.Y., and S.Z. wrote the paper.

The authors declare no conflict of interest.

*This Direct Submission article had a prearranged editor.

Freely available online through the PNAS open access option.

See Commentary on page 5143.

[1]To whom correspondence should be addressed. E-mail: slobodan.zumer@fmf.uni-lj.si.

This article contains supporting information online at www.pnas.org/lookup/suppl/doi:10.1073/pnas.1015831108/-/DCSupplemental.

Three-Dimensional Colloidal Crystals

To identify the energetically favorable trapping sites we calculate the free energy density using a mean field Landau–de Gennes approach (31). Indeed, a single defect line can generate trapping potentials as strong as approximately 200 kT for 30 nm particles, but also regular arrays of defect lines in chiral nematics (32). Fig. 1 shows isosurfaces of constant free energy density (green) and the network of disclination lines (red) within each of the blue phase unit cells. The free energy density is largest in the core regions of the defects and drops substantially within the double-twist regions. The positions of the maxima in the free energy density reflect the cubic symmetry of the blue phase texture, so that the trapping potential for the colloids also reflects this symmetry allowing crystalline arrangements of colloids to form.

Stable 3D colloidal crystals in BP I and BP II are shown in Fig. 2 *A–D*. For simplicity, we choose particles including spherically symmetric homeotropic surface alignment. Structures vary in the number of particles per unit cell, and correspond to regular crystalline configurations that can be stabilized by the symmetry provided by the blue phase defect pattern. In all structures, the particles are individually trapped to effective trapping sites. The structures are built by positioning a given number of particles per unit cell (one, two, and four) into predetermined symmetric trapping sites identified from the free energy density profile of the BPs, and then let to fully equilibrate with respect to the particle positions, size of the unit cell, and texture of the BP. All shifts of particles from the symmetric positions lead to an increase in free energy confirming that the crystalline arrangements are energetically preferred.

To identify the equilibrium lattice, free energies of various BP colloidal crystals relative to the FCC (BP I) and BCC (BP II) are shown in Fig. 3 *A* and *B*. Interestingly, in BP I, we find that the arrangement with lowest free energy is the FCC crystal (Fig. 2*A*) for the majority of particle sizes (smaller than approximately 100 nm) and BCC for larger particles. Qualitatively, one can explain this change by an effectively smaller filling fraction in BCC crystals, which at larger particle sizes allows for more efficient relaxation of liquid crystal deformation imposed by surface anchoring. In BP II, the energetically most favorable structure is BCC colloidal crystal (Fig. 2*C*). The free energy differences per unit cell between various lattices are typically larger than $\sim 10\ k_B T$ in BP I and larger than a few $k_B T$ in BP II. In BP I the relatively large energy differences indicate favoring of a single (FCC or BCC) lattice, whereas in BP II the BCC and single cubic

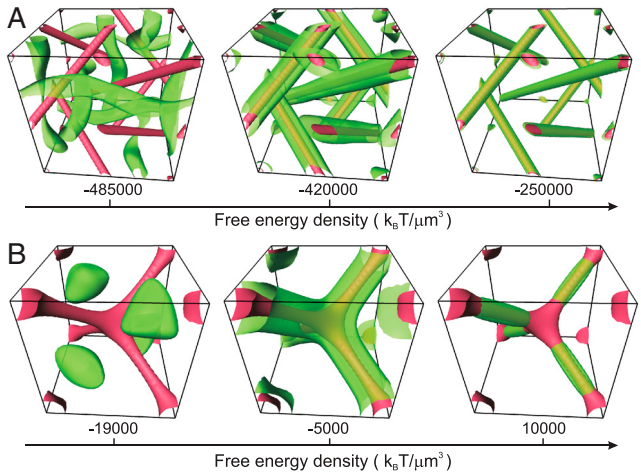

Fig. 1. Local free energy density profile. (*A*) BP I. (*B*) BP II. Isosurfaces of the free energy density are shown in green. Disclination lines are drawn in red as isosurfaces of the nematic degree of order $S = 0.23$ (BP I) and $S = 0.1$ (BP II). Regions with the highest free energy density coincide with the centers of the defect lines and represent the optimum location for colloidal inclusions.

(SC) lattice will compete, possibly forming polydomains. Finally, we should stress that the free energy differences between various lattices also depend on surface anchoring and on LC material parameters, therefore a particular choice of materials may energetically favor another crystalline structure (Fig. 2 *B* and *D*).

Experimentally, our process to generate colloidal crystals corresponds to forming particles in situ, which we propose could actually be achieved by phase separation of chiral nematic and the second component. Building on the work of Loudet et al in nematic phase (33), one could perform temperature quench within the blue phase to trigger phase separation and form particles—droplets—of the second component, now ideally at the optimal trapping sites. Such a process could avoid clustering and formation of irregular metastable structures, which is otherwise typically observed when introducing particles into defect structures of liquid crystal (24). Being able to control uniform dispersion of particles, an alternative to phase separation could be to use isotropic to cholesteric transition, allowing particles to move only when the blue phase defect pattern is fully established.

Fluctuations of particles between effective trapping sites in the blue phase pattern could break the crystalline order of particles. To address the role of fluctuations, free energy barriers between the trapping sites are calculated. They prove to be strongly anisotropic and have easy directions (with lowest increase in energy) always along disclination lines. The height of energy barriers increases with particle size and is for 50 nm particles $\sim 10\ k_B T$ along easy directions in both BP I and BP II. For smaller particles (approximately 10 nm), this height of the energy barriers indicates that thermal fluctuations can cause fluctuations in particle positions and also migration of particles along disclinations, whereas for larger particles (approximately 100 nm), fluctuations are insufficient to cause changes in the structure. Another mechanism that could affect the regularity of colloidal crystals is clustering of multiple particles in a single trapping site. Performing the analysis in BP II, we compared the configuration to one trapping site crowded by two particles and conversely one empty site, with the regular crystalline BCC structure. The crowded configuration was found to have $\sim 10\ k_B T$ higher free energy, implying that such crowding is energetically not favorable, because particles cannot optimally cover the disclination regions. To relate our work to studies of entropy-driven depletion forces that are technologically commonly used to achieve aggregation and crowding, they are generically small when compared to liquid crystalline effective elastic forces because in blue phase colloids the separation between particles is typically at the scale of particles (approximately 100 nm) and not liquid crystal molecules (approximately 0.1 nm) (34, 35). Finally, the particle aggregation can be affected by the particle–liquid crystal interfacial tension, yet this behavior is strongly dependent on the specific choice of materials. Our work is only relevant for materials that give total wetting at the surfaces of particles where the interfacial tension can be ignored. Namely, for totally wetted surfaces, the surface area and therefore the surface tension energy remain unchanged no matter the positioning or aggregation of particles. However, for typical materials, an estimate of the surface tension energy F_s gives $F_s = 4\pi\gamma r^2 \sim 10^{-15}$ J [$\gamma \sim 0.03$ N/m^2 is typical surface tension of LCs (36) and $r \sim 50$ nm is typical particle radius], which is in similar to characteristic liquid crystalline energies of blue phase unit cells (*Materials and Methods*). Therefore, surface tension can profoundly affect the particle aggregation.

Fig. 4 *A* and *B* shows the free energy, relative to a colloid-free texture, as a function of the particle radius for a range of anchoring strengths W. When W is weak, $W \lesssim 10^{-5}$ Jm^{-2}, the free energy is steadily reduced by increasing the particle size. In this regime, particles stabilize the BP texture. The effect is largest for weak anchoring and relatively large particle radius, $r \sim 100$ nm. When the surface anchoring is strong, the distortions

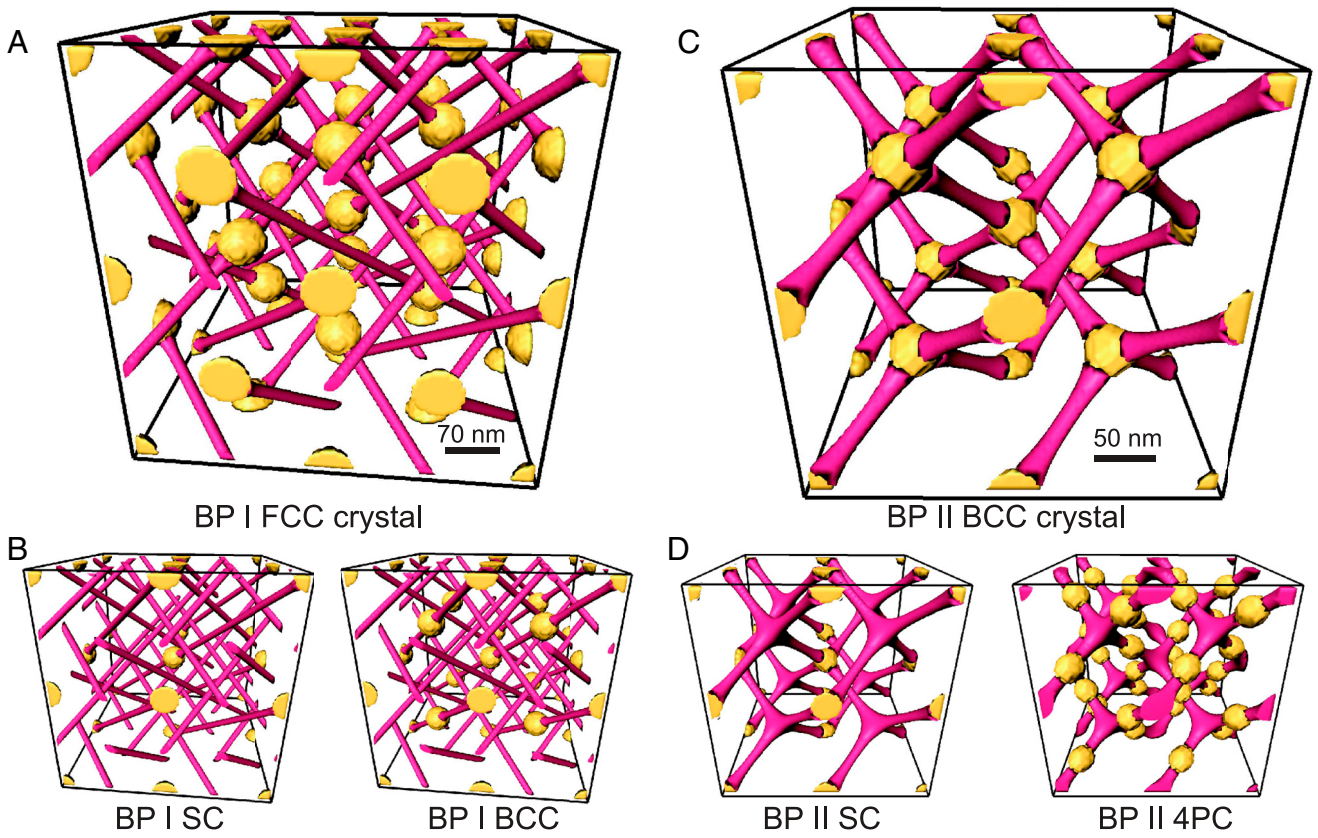

Fig. 2. Three-dimensional BP colloidal crystals. (*A*) Energetically favorable FCC colloidal crystal in BP I, (*B*) stable colloidal crystals in BP I with simple cubic (SC) and BCC unit cell, (*C*) the most energetically favorable BCC colloidal crystal in BP II, and (*D*) stable colloidal crystals in BP II with SC and four particle configuration (4PC) unit cell. In BP I, disclination lines are drawn as isosurfaces of degree of order $S = 0.23$ ($S_{bulk} = 0.40$), particle radius is $r = 70$ nm. In BP II, disclination lines are visualized as isosurfaces of $S = 0.1$ ($S_{bulk} = 0.26$), $r = 50$ nm. In all cases $2 \times 2 \times 2$ unit cells have been shown to better illustrate the structure.

induced in the BP texture are substantial and the overall free energy is increased by the addition of the particles.

Fig. 4 *C* and *D* shows how the unit cell size of BP colloidal crystals depends on the particle size. In both BPs, the unit cell shrinks for small particles and expands for larger particles, with a quadratic dependence fitting the numerical results well. This behavior may be understood if we recall that the energetic cost of the disclinations pushes the double-twist cylinders apart, making the unit cell in a colloid-free BP larger than the chirality alone would prefer (37). The removal of part of this cost allows the double-twist cylinders to pack more closely, reducing the lattice constant. However, if the colloid radius r is larger than the effective core of the disclination, it will force the double-twist cylinders further apart, and increase the size of the BP unit cells. Effectively, these changes of the effective thickness of double-twist cylinders cause the change in volume of the unit cell to scale as $\Delta V \sim r(r - 2\tilde{\xi})$, with a minimum for $r = \tilde{\xi}$ at particle sizes comparable to the disclination core size $\tilde{\xi}$. The core size $\tilde{\xi}$ is proportional to the nematic correlation length ξ, giving typically $\xi \propto \tilde{\xi} \sim 10$ nm.

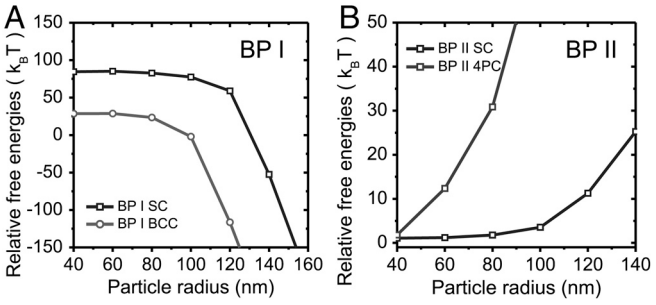

Fig. 3. Relative free energies of various crystalline lattices as functions of particle radii relative to FCC lattice and BCC lattice in (*A*) BP I and (*B*) BP II, respectively.

Increasing Thermodynamic Stability of Blue Phases

The reduction in free energy afforded by immersing colloidal particles offers an appealing mechanism for increasing the thermodynamic stability of BPs. In Fig. 5 we show the phase diagram for colloidal blue phases, calculated numerically for 100 nm radius particles with weak homeotropic anchoring ($W = 10^{-5}$ J/m^2) and taking FCC colloidal crystals in BP I and BCC colloidal crystals in BP II. The cholesteric–colloidal BP I phase boundary was estimated using an undistorted cholesteric texture and hence corresponds to an absolute upper limit. The effect of particles is pronounced, yielding a significant increase in the stability of both BP II relative to BP I and of BP I relative to the cholesteric For example, for BP II with particles, at a typical inverse pitch of $1/p_0 = 2$ μm^{-1}, the temperature range increases by a factor of approximately three.

The general change in free energy caused by the colloids may be understood from scaling arguments. Each colloid removes a portion of the disclination network proportional to its radius, leading to a free energy savings on the order of Kr. The surface anchoring leads to a free energy cost on the order of Wr^2, giving a net change in the energy of $\sim -aKr + bWr^2$, where a and b are positive constants. However, the particles also affect the size of the BP unit cell giving a term associated with the work done, $-p\Delta V$, where p is an effective pressure for the change in volume $\Delta V \sim r(r - 2\tilde{\xi})$. The complete scaling of the free energy then takes the form $\Delta F = (-aK + 2pc\tilde{\xi})r + (bW - pc)r^2$, where c is another positive constant, and this scaling is in good agreement

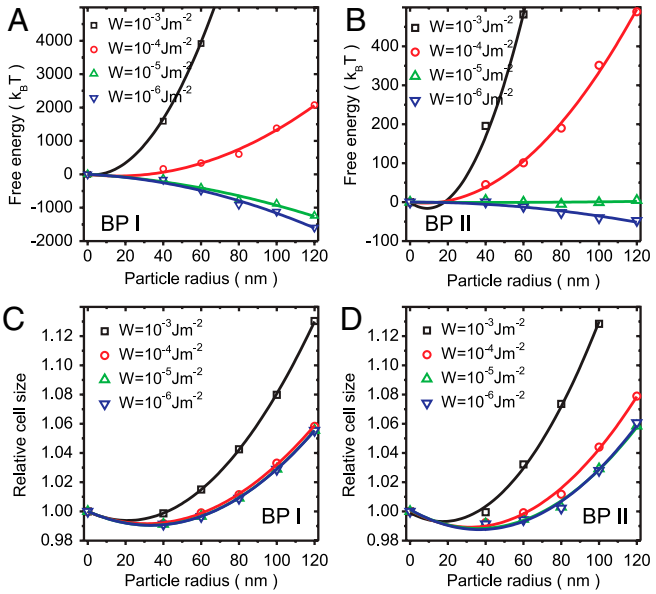

Fig. 4. Free energy profile for various particle sizes and anchoring strengths W in (*A*) BP I FCC colloidal crystals and (*B*) BP II BCC colloidal crystals. Relative unit cell sizes for various particle sizes and anchoring strengths of (*C*) BP I FCC colloidal crystal and (*D*) BP II BCC colloidal crystal. Particle radius $r = 0$ corresponds to BP with no particles. Free energy and relative cell size profiles for $W = 10^{-6}$ J/m^2 change for less than 2% and 0.01%, respectively, upon further decreasing the anchoring strength ($W \to 0$).

with the numerical results in Fig. 2. By optimizing the regime of negative ΔF, one maximizes the phase stabilization of blue phases.

Discussion

To stabilize the blue phases, we expect it to be energetically favorable to use numerous small (nano-sized) particles, as they can more effectively fill the defect cores and reduce the total free energy. Even more effective filling of the defects could be achieved by using anisotropic particles, e.g., ellipsoids or spherocylinders. As the relative metastability of the different crystalline structures is dependent on particle size, an interesting approach would be to use electro- or thermo-responsive particles (38), which may allow for a reconfiguration of the crystalline structures by continuously changing the particle size. Based on the free energy profile of BP II (Fig. 1*B*), we speculate that the body-centered cubic configuration (Fig. 2*C*) could transform into the four particle configuration (Fig. 2*D*, *Right*) upon reducing the size of the particles. Furthermore, changing the particle size continuously would also provide an isotropic expansion or contraction of the blue phase unit cell, with technological interest as a tunable resonator in lasing applications (39). Indeed, in comparison to usual solid state resonators, liquid crystal-based microresonators have proven to exhibit large Q factors and two orders of magnitude larger tunability (40). Finally, we mention that the use of fluorescently labeled colloids could enable a means of directly studying the structure of the blue phases (41) and of following the kinetics of textural rearrangements (42, 43) and blue phase rheology (44).

The important step beyond our work is the kinetics of blue phase colloids, as the formation of perfect colloidal crystals will have to compete with random arrangements and possible phase separation into colloid-rich and colloid poor regions. In addition, it is a priori uncertain that a BP nucleating from an isotropic phase dispersed with colloids will form the same cubic lattices that it does in the absence of particles. Thus, there is ample motivation for studying the kinetic aspects of colloidal particles in BPs, addressing domain growth (45), possible thermal annealing, and external fields assisted assembly.

In summary, we have demonstrated that 3D colloidal crystals can be assembled in LC blue phases by using the free energy gain of trapping the particles in the core regions of defect lines. The universality of this mechanism opens routes for self-assembly. Equilibrium configurations of FCC colloidal crystals in BP I and BCC colloidal crystals in BP II were identified as being energetically most favorable. The effects of particle size and surface anchoring properties were addressed, as main material tunability parameters. Two specific roles were identified: Colloidal particles with weak surface anchoring increase the thermodynamic stability of BPs and larger particles and stronger surface anchoring give stronger binding of particles to the trapping sites in BPs. However, both the size of particles and surface anchoring affect the 3D profile of 3D trapping sites, which can change the relative metastability of various possible particle lattices. In a wider context, our results open a unique direction for the assembly of complex 3D optical structures and their possible application in photonics and plasmonics. Moreover, ordering and stabilization of complex chiral spatial 3D fields bring our results in close relation to other chiral condensed matter systems, including skyrmions and superconductive vortices.

Materials and Methods

To model blue phase colloids, we employ a continuum, mean field Landau–de Gennes approach based upon the tensor order parameter, Q_{ij}. This approach naturally accounts for effective elasticity of the liquid crystal, variations in the magnitude of the order, and possible biaxiality. The free energy is taken to be

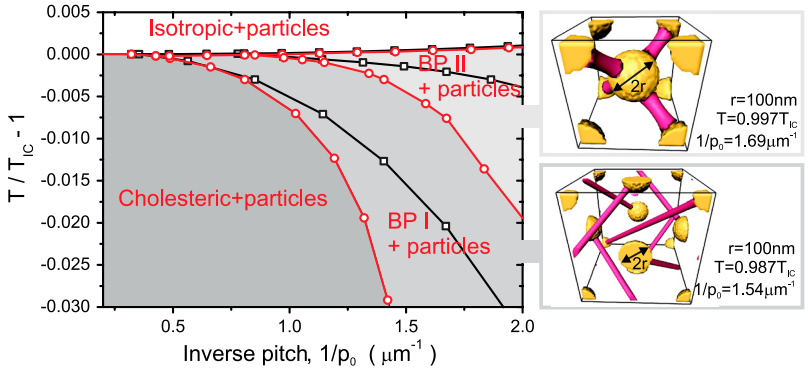

Fig. 5. BP phase stabilization by particle doping. (*Left*) Phase diagram of BP colloidal crystals in terms of inverse cholesteric pitch $1/p_0$ and temperature T (T_{IC} is isotropic-cholesteric transition temperature). Red lines are phase boundaries of the BP with immersed colloidal particles (homeotropic anchoring $W_0 = 10^{-4}$ J/m^2). Black lines show phase boundaries of the chiral LC with no particles. Note the large increase in the phase space of the BP region when particles are introduced. (*Right*) Shows examples of corresponding BP colloidal crystals at specific temperature and inverse pitch.

$$F = \int_{LC} \left\{ \frac{A_0(1-\gamma/3)}{2} Q_{ij}Q_{ij} - \frac{A_0\gamma}{3} Q_{ij}Q_{jk}Q_{ki} + \frac{A_0\gamma}{4} (Q_{ij}Q_{ij})^2 \right\} dV + \int_{LC} \left\{ \frac{L}{2} \frac{\partial Q_{ij}}{\partial x_k} \frac{\partial Q_{ij}}{\partial x_k} + 2q_0 L \epsilon_{ikl} Q_{ij} \frac{\partial Q_{lj}}{\partial x_k} \right\} dV + \int_{CS} \left\{ \frac{W}{2} (Q_{ij} - Q_{ij}^0)(Q_{ij} - Q_{ij}^0) \right\} dS, \quad [1]$$

where LC denotes an integral over the volume occupied by the liquid crystal only and colloidal surfaces (CS) over the surfaces of the colloidal particles. The first term is the bulk free energy and describes a first order transition (at $\gamma = 2.7$) between an isotropic and a nematic phase, with A_0 a constant with the dimensions of an energy density and γ an effective dimensionless temperature. The second term describes the energy cost of distortions in the liquid crystalline order; L is an elastic constant, q_0 is a chiral parameter related to the pitch of the cholesteric helix by $p = 2\pi/q_0$ and ϵ_{ikl} is the fully antisymmetric alternating tensor equal to $+1(-1)$ if i, k, l is an even (odd) permutation of one, two, three, and zero otherwise. The final term describes the interaction of the liquid crystal with the surfaces of the colloids, where W represents the strength of the surface anchoring and Q_{ij}^0 is the order parameter preferred by the surface, which we take to be homeotropic. The equilibrium surface and bulk profile of the order parameter tensor is qualitatively unchanged in the most relevant regime of weak anchoring.

We obtained minimum energy configurations by solving a system of coupled partial differential equations with appropriate boundary conditions using an explicit Euler finite difference relaxation algorithm on a cubic mesh. To produce the desired blue phase texture, initial conditions were chosen for the tensor Q_{ij} corresponding to analytic expressions in the high chirality limit ($q_0 \to \infty$). The surface of each particle is defined by the set of mesh points contained within a spherical shell with thickness equal to the mesh resolution. Mesh points outside the surface are updated according to the bulk Ginzburg–Landau equations, appropriate boundary conditions are imposed on the surface points and no computations are performed for the interior points. For computational efficiency, the effects of fluid flow are neglected in the relaxational dynamics as these are not expected to effect the equilibrium configurations.

Material parameters were chosen to match a typical cholesteric nematic liquid crystal and, if not stated differently, were taken to be: $L = 2.5 \times 10^{-11}$ N, $A_0 = 1.02 \times 10^5$ J/m^3, $W = 10^{-4}$ J/m^2, ($\gamma = 3.375$, $p_0 = 0.566$ μm) in BP I, and ($\gamma = 2.755$, $p_0 = 0.616$ μm) in BP II.

ACKNOWLEDGMENTS. M.R. acknowledges support of the European Commission (EC) under the Marie Curie Program Active Liquid Crystal Colloids, content reflects only the authors views and not the views of the EC. G.P.A. thanks Randall Kamien for discussions and acknowledges funding from National Science Foundation Grant DMR05-47320. M.R. and S.Z. acknowledge funding from Slovenian Research Agency P1-0099, J1-2335, FP7 215851-2 Hierarchy, and Center of Excellence Advanced Materials and Technologies for the Future.

1. Hellweg T (2009) Towards large-scale photonic crystals with tuneable band gaps. *Angew Chem Int Ed* 48:6777–6778.
2. Hornreich RM, Shtrikman S, Sommers C (1994) Photonic band gaps in body-centered-cubic structures. *Phys Rev B: Condens Matter Mater Phys* 49:10914–10917.
3. Tanaka Y, et al. (2007) Dynamic control of the Q factor in a photonic crystal nanocavity. *Nat Mater* 6:862–865.
4. Yao J, et al. (2008) Optical negative refraction in bulk metamaterials of nanowires. *Science* 321:930–930.
5. Won R (2009) Photonic crystals on a chip. *Nat Photonics* 3:498–499.
6. Kang D, et al. (2001) Electro-optic behavior of liquid-crystal-filled silica opal photonic crystals: Effect of liquid-crystal alignment. *Phys Rev Lett* 86:4052–4055.
7. Israelachvili JN (2011) *Intermolecular and Surface Forces* (Elsevier, Oxford).
8. Pishnyak OP, et al. (2007) Levitation, lift, and bidirectional motion of colloidal particles in an electrically driven nematic liquid crystal. *Phys Rev Lett* 99:127802.
9. Miguez H, et al. (1998) Control of the photonic crystal properties of fcc packed submicrometric SiO_2 spheres by sintering. *Adv Mater* 10:480–483.
10. Van Blaaderen A, Ruel R, Wiltzius P (1997) Template-directed colloidal crystallization. *Nature* 385:321–324.
11. Leunissen ME, et al. (2005) Ionic colloidal crystals of oppositely charged particles. *Nature* 437:235–240.
12. Hynninen A-P, Thijssen JHJ, Vermolen ECM, Dijkstra M, Van Blaaderen A (2007) Self-assembly route for photonic crystals with a bandgap in the visible region. *Nat Mater* 6:202–205.
13. Nykypanchuk D, Maye MM, van der Lelie D, Gang O (2008) DNA-guided crystallization of colloidal nanoparticles. *Nature* 451:549–552.
14. Poulin P, Stark H, Lubensky TC, Weitz DA (1997) Novel colloidal interactions in anisotropic fluids. *Science* 275:1770–1773.
15. Yada M, Yamamoto J, Yokoyama H (2004) Direct observation of anisotropic interparticle forces in nematic colloids with optical tweezers. *Phys Rev Lett* 92:185501.
16. Ravnik M, et al. (2007) Entangled nematic colloidal dimers and wires. *Phys Rev Lett* 99:247801.
17. Musevic I, et al. (2006) Two-dimensional nematic colloidal crystals self-assembled by topological defects. *Science* 313:954–958.
18. Min Y, Akbulut M, Kristiansen K, Golan Y, Israelachvili J (2008) The role of interparticle and external forces in nanoparticle assembly. *Nat Mater* 7:527–538.
19. Coles HJ, Pivnenko MN (2005) Liquid crystal "blue phases" with a wide temperature range. *Nature* 436:997–1000.
20. Castles F, Morris SM, Terentjev EM, Coles HJ (2010) Thermodynamically stable blue phases. *Phys Rev Lett* 104:157801.
21. Kikuchi H, Yokota M, Hisakado Y, Yang H, Kajiyama T (2002) Polymer-stabilized liquid crystal blue phases. *Nat Mater* 1:64–68.
22. Muhlbauer S, et al. (2009) Skyrmion lattice in a chiral magnet. *Science* 323:915–919.
23. Wright DC, Mermin ND (1989) Crystalline liquids—the blue phases. *Rev Mod Phys* 61:385–432.
24. Zapotocky M, et al. (1999) Particle-stabilized defect gel in cholesteric liquid crystals. *Science* 283:209–212.
25. Pires D, Fleury J-B, Galerne Y (2007) Colloid particles in the interaction field of a disclination line in a nematic phase. *Phys Rev Lett* 98:247801.
26. Fleury J-B, Pires D, Galerne Y (2009) Self-connected 3-D architecture of microwires. *Phys Rev Lett* 103:267801.
27. Voloschenko D, et al. (2002) Effect of director distortions on morphologies of phase separation in liquid crystals. *Phys Rev E: Stat Nonlinear Soft Matter Phys* 65:060701(R).
28. Yoshida H, et al. (2009) Nanoparticle-stabilized cholesteric blue phases. *Appl Phys Express* 2:121501.
29. Karatairi E, et al. (2010) Nanoparticle-induced widening of the temperature range of liquid-crystalline blue phases. *Phys Rev E: Stat Nonlinear Soft Matter Phys* 81:041703.
30. Fukuda J (2010) Stabilization of a blue phase by a guest component: An approach based on a Landaude Gennes theory. *Phys Rev E: Stat Nonlinear Soft Matter Phys* 82:061702.
31. Alexander GP, Yeomans JM (2006) Stabilizing the blue phases. *Phys Rev E: Stat Nonlinear Soft Matter Phys* 74:061706.
32. Ravnik M, Alexander GP, Yeomans JM, Zumer S (2010) Mesoscopic modelling of colloids in chiral nematics. *Faraday Discuss* 144:159–169.
33. Loudet J-C, Barois P, Poulin P (2000) Colloidal ordering from phase separation in a liquidcrystalline continuous phase. *Nature* 407:611–613.
34. Kaplan PD, Faucheux LP, Libchaber AJ (1994) Direct observation of the entropic potential in a binary suspension. *Phys Rev Lett* 73:2793–2796.
35. Roth R, Evans R, Dietrich S (2000) Depletion potential in hard-sphere mixtures: Theory and applications. *Phys Rev E: Stat Nonlinear Soft Matter Phys* 62:5360–5377.
36. Gannon MGJ, Faber TE (1978) The surface tension of nematic liquid crystals. *Philos Mag A* 37:117–135.
37. Grebel H, Hornreich RM, Shtrikman S (1983) Landau theory of cholesteric blue phases. *Phys Rev A: At Mol Opt Phys* 28:1114–1138.
38. Debord SB, Lyon LA (2003) Influence of particle volume fraction on packing in responsive hydrogel colloidal crystals. *J Phys Chem B* 107:2927–2932.
39. Cao W, Muńoz A, Palffy-Muhoray P, Taheri B (2002) Lasing in a three-dimensional photonic crystal of the liquid crystal blue phase II. *Nat Mater* 1:111–113.
40. Humar M, Ravnik M, Pajk S, Musevic I (2009) Electrically tunable liquid crystal optical microresonators. *Nat Photonics* 3:595–600.
41. Higashiguchi K, Yasui K, Kikuchi H (2008) Direct observation of polymer-stabilized blue phase I structure with confocal laser scanning microscope. *J Am Chem Soc* 130:6236–6327.
42. Kitzerow H-S (1991) The effect of electric fields on blue phases. *Mol Cryst Liq Cryst* 202:51–83.
43. Alexander GP, Marenduzzo D (2008) Cubic blue phases in electric fields. *Europhys Lett* 81:66004.
44. Dupuis A, Marenduzzo D, Orlandini E, Yeomans JM (2005) Rheology of cholesteric blue phases. *Phys Rev Lett* 95:097801.
45. Henrich O, Stratford K, Marenduzzo D, Cates ME (2010) Ordering dynamics of blue phases entails kinetic stabilization of amorphous networks. *Proc Natl Acad Sci USA* 107:13212–13215.